4490–4498 *Nucleic Acids Research, 2011, Vol. 39, No. 10* *Published online 3 February 2011*
doi:10.1093/nar/gkr029

Zn^{2+} selectively stabilizes FdU-substituted DNA through a unique major groove binding motif

Supratim Ghosh[1,2], Freddie R. Salsbury Jr[3], David A. Horita[4] and William H. Gmeiner[1,2,*]

[1]Department of Cancer Biology, [2]Program in Molecular Genetics, Wake Forest University School of Medicine, Winston-Salem, NC 27157, [3]Department of Physics, Wake Forest University, Winston-Salem, NC 27109 and [4]Department of Biochemistry, Wake Forest University School of Medicine, Winston-Salem, NC 27157, USA

Received September 22, 2010; Revised January 10, 2011; Accepted January 13, 2011

ABSTRACT

We report, based on semi-empirical calculations, that Zn^{2+} binds duplex DNA containing consecutive FdU–dA base pairs in the major groove with distorted trigonal bipyramidal geometry. In this previously uncharacterized binding motif, O4 and F5 on consecutive FdU are axial ligands while three water molecules complete the coordination sphere. NMR spectroscopy confirmed Zn^{2+} complexation occurred with maintenance of base pairing while a slight hypsochromic shift in circular dichroism (CD) spectra indicated moderate structural distortion relative to B-form DNA. Zn^{2+} complexation inhibited ethidium bromide (EtBr) intercalation and stabilized FdU-substituted duplex DNA ($\Delta T_m > 15^{\circ}C$). Mg^{2+} neither inhibited EtBr complexation nor had as strong of a stabilizing effect. DNA sequences that did not contain consecutive FdU were not stabilized by Zn^{2+}. A lipofectamine preparation of the Zn^{2+}–DNA complex displayed enhanced cytotoxicity toward prostate cancer cells relative to the individual components prepared as lipofectamine complexes indicating the potential utility of Zn^{2+}–DNA complexes for cancer treatment.

INTRODUCTION

Zinc has a unique role among metals in regulating the normal function of the prostate gland. Further, the sensitivity of prostatic adenocarcinoma (PCa) cells to Zn^{2+}, particularly in combination with chemotherapy, represents a potentially highly selective approach to prostate cancer treatment (1,2). Zn^{2+} forms high-affinity complexes with biopolymers, most notably the Zn^{2+}-finger motif that is widely used by transcription factors for sequence-specific DNA recognition. These peptidic motifs frequently have subnanomolar affinity for Zn^{2+} and presumably persist in cellular environments in which the free Zn^{2+} concentration is extremely low (3). Zn^{2+} has also been reported to form specific complexes with DNA with some reports indicating that Zn^{2+} can mediate base pair formation, particularly for nucleobases with acidic imino hydrogens such as 5-fluorouracil (5FU) (4,5). In principle, Zn^{2+} complexed to 5-fluoro-2′-deoxyuridine (FdU)-substituted DNA could be useful for cancer treatment in light of the cytotoxic properties of FdUMP[10] (6–8).

The structural motif responsible for Zn^{2+} complexation by FdU-substituted DNA is not presently known. Previous reports indicated that Zn^{2+} interacted with N3 of deprotonated FdU forming an ionic base pair with dA similar in geometry to Watson–Crick (4,5). These studies were performed using DNA sequences with alternating FdU and 2′-deoxyadenosine (dA) nucleotides. Subsequent studies using FRET revealed DNA aggregation occurred under similar conditions (9). In the present report, we demonstrate that Zn^{2+}, but not Mg^{2+}, selectively stabilizes DNA containing consecutive FdU–dA base pairs. The Zn^{2+} complexes were characterized by enhanced thermal stability and exclusion of ethidium bromide (EtBr). Zn^{2+}-mediated stabilization occurs only for DNA sequences containing consecutive FdU–dA base pairs and is not observed for sequences that do not contain FdU or that contain alternating FdU–dA nucleotides.

In the present studies, semi-empirical and *ab initio* calculations were used to determine the energetically preferred geometry for Zn^{2+} binding to DNA sequences containing consecutive FdU nucleotides (Figure 1). Although crystallographic and NMR studies have indicated a propensity for monovalent cations to occupy the deep, narrow minor groove of A-tract DNA sequences (10,11), the calculations revealed a distinct minimum energy conformation for the FdU–dA dimer complexed with Zn^{2+} under conditions when the 5′-terminal FdU was deprotonated. In this low energy structure, Zn^{2+} is localized in the major groove and interacts with F5 from the 5′-terminal FdU and with O4 from the 3′-terminal

*To whom correspondence should be addressed. Tel: +1 336 716 6216; Fax: +1 336 716 0255; Email: bgmeiner@wfubmc.edu

FdU as axial ligands in a distorted trigonal bipyramidal geometry with three water molecules occupying the equatorial sites. This previously uncharacterized structural motif is consistent with all of the spectroscopic, as well as the computational data.

We also evaluated the cytotoxicity of the Zn^{2+}–DNA complex to determine to what extent the inclusion of Zn^{2+} in FdU-substituted DNA complexes may be useful for prostate cancer treatment. The Zn^{2+}–DNA complex was prepared using lipofectamine both to stabilize the complex under cell culture conditions and to improve cellular uptake. The results clearly demonstrate that the DNA–Zn^{2+} complex has greater cytotoxicity toward PCa cells than either DNA alone or Zn^{2+} alone. Thus, our results demonstrate that Zn^{2+} interacts with DNA containing consecutive FdU–dA base pairs by binding in the major groove in a previously uncharacterized structural motif. Further, complexation of Zn^{2+} enhances the cytotoxicity of FdU-substituted DNA toward PCa cells demonstrating the feasibility for using this structural motif for PCa treatment.

MATERIALS AND METHODS

Design and synthesis of DNA hairpins

The DNA sequences used for these studies were designed to favor intramolecular hairpin formation and to be stable at physiological temperature. Each of the four hairpin DNA sequences consisted of a 10 bp stem consisting of all A–T (or A–FdU) base pairs. The loop region included the GAA sequence that was previously shown to promote hairpin formation (12). The loop was closed by a single C–G base pair. Gel-electrophoresis studies (15% native PAGE gel) demonstrated a single species was present (Supplementary Figure S8) and subsequent ^{1}H NMR studies demonstrated the chemical shift characteristic for the C–G base pair closing the loop in a similar sequence (13). Four DNA hairpins were designed (Figure 2). The sequence 'A10–T10' included 10 consecutive T nucleotides at the 5′-terminus and the corresponding 10 consecutive A nucleotides at the 3′-terminus. The '5′-FdU' sequence was identical to the A10–T10 sequence except all of the T nucleotides were substituted by FdU. The '3′-FdU' hairpin DNA sequence had the location of the 10 consecutive A and FdU nucleotides reversed relative to the 5′-FdU hairpin with the 10 consecutive FdU nucleotides located at the 3′-terminus. The 'Alt-FdU' sequence had alternating A and FdU nucleotides throughout the stem and thus lacked consecutive FdU nucleotides. These DNA hairpin sequences were designed to evaluate the structural requirements for FdU substitution on formation of complexes with divalent metal ions, including Zn^{2+} and Mg^{2+}. All DNA sequences were prepared at the University of Calgary DNA Core laboratory and purified by gel-filtration chromatography.

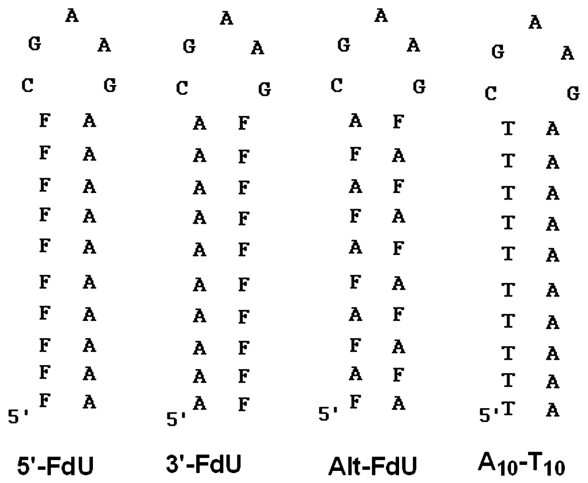

Figure 2. Structure of the DNA hairpins investigated in the present studies. Each of the hairpins includes a 10 bp stem capped by the pentanucleotide CGAAG to promote intramolecular hairpin formation. The control sequence A10–T10 consists of all native nucleotides. The three FdU-containing sequences differ in the location of FdU nucleotides as shown.

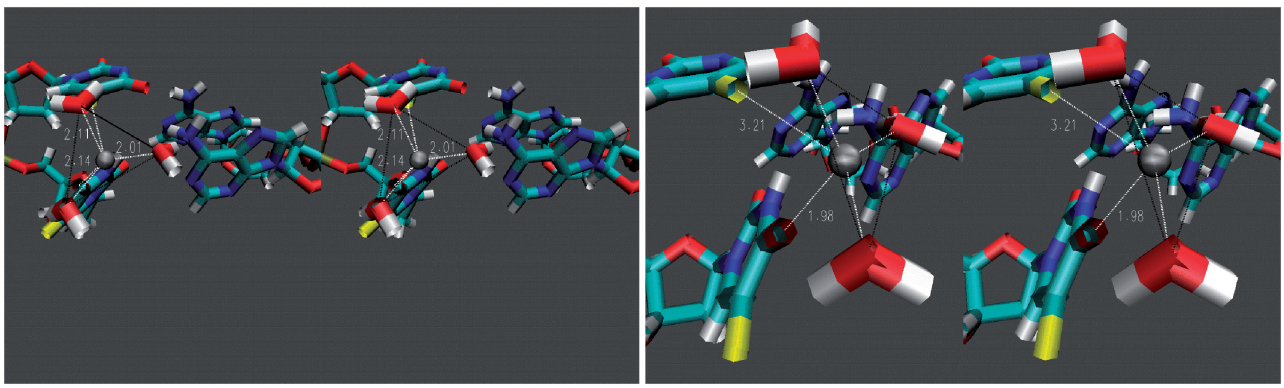

Figure 1. Computationally derived model of Zn^{2+} complexation to the hemi-deprotonated dimeric duplex consisting of consecutive FdU–dA base pairs. Zn^{2+} is located in the major groove with a distorted trigonal bipyramidal geometry in which the fluorine from the deprotonated FdU is one axial ligand and O4 from the second FdU is the second axial ligand. Water molecules are the equatorial ligands. White dashed lines are used to illustrate the coordinating atoms. (**A**) View emphasizing the Zn^{2+}–water interactions; (**B**) View emphasizing Zn^{2+} interactions with DNA nucleobases. The triangle connecting the three water oxygens provides a visual frame of reference.

Formation of Zn^{2+}–DNA complexes

Intramolecular hairpins were formed using 1 mM DNA in dH_2O by heating to 80°C for 5 min followed by rapid cooling. Zn^{2+} (or Mg^{2+}) complexes were formed by incubating 100 μM DNA with 0–5 mM $ZnCl_2$ (or $MgCl_2$) in M-DNA buffer (20 mM sodium cacodylate, pH 8.0, 10 mM NaCl) for 1 h at room temperature. The formation of specific Zn^{2+} complexes with hairpin DNA sequences was evaluated using an EtBr exclusion fluorescence assay as previously described (5). This assay was performed by combining 20 μl of the above described M-DNA complex with 80 μl of EtBr solution (10 mM NaCl, 20 mM sodium cacodylate, pH 8.0, +25 μM EtBr) followed by incubation for 30 min at room temperature in a 96-well clear bottom, black plate (Costar). The final divalent metal concentration ranged from 0 to 1 mM. EtBr fluorescence was detected using a Typhoon-9210 variable mode imager with Green laser (532 nm) excitation and 610 nm emission filter (with 500 PMT set). Fluorescence intensity was quantified with the software ImageQuant 5.2 and graphed versus Zn^{2+}/Mg^{2+} concentration.

Analytical characterization of DNA–Zn^{2+} complexes

DNA–Zn^{2+} complexes were analyzed by circular dichroism (CD) and NMR spectroscopy to characterize their structural features and any specific changes induced by Zn^{2+} or Mg^{2+}. A 300 μl aliquot of 20 μM DNA solution with either 0, 0.5 mM, 1 mM Zn^{2+} (or Mg^{2+}) was prepared in M-DNA buffer as described above and used to obtain the CD spectrum. An Aviv CD spectrometer was used to scan the region from 210 to 310 nm at a rate of 0.5 nm/s. Temperature was controlled at 20°C.

^{1}H, ^{19}F, ^{31}P and ^{13}C NMR spectroscopy were used to investigate specific structural perturbations induced by Zn^{2+} to the 3′-FdU hairpin. For the NMR analysis, 500 μl of 0.5 mM 3′-FdU in M-DNA buffer modified to contain 40 mM sodium cacodylate were used. NMR samples contained either no metal, 5 mM Zn^{2+} or 5 mM Mg^{2+}. Also, 10% D_2O was included to maintain lock. The final pH of the samples was adjusted to either pH 7 or 8 (±0.1 pH unit). ^{1}H NMR spectra were collected using a Bruker Avance DRX 600 MHz spectrometer with a TXI Cryoprobe at 10°C using the WATERGATE sequence with a 3-9-19 refocusing pulse. Nulls were set at ±18.1 ppm. Spectra were acquired with a spectral width of 33.3 ppm, 8192 total data points and 256 scans. A relaxation delay of 10 s was used to obtain ^{1}H spectra for integration. ^{13}C spectra were collected at 15°C using inverse-gated proton decoupling during acquisition, a 2 s relaxation delay, a spectral width of 200.0 ppm, 8192 total data points and 65,536 scans (30° pulse). ^{19}F and ^{31}P NMR spectra were acquired using a Bruker 300 MHz NMR instrument with 85% H_3PO_4 ($\delta = 0$ ppm) or 5 mM aqueous solution of KF ($\delta = 125.3$ ppm) as concentric internal standard capillaries (Wilmad).

Temperature-dependant melting analysis

Temperature-dependent melting (T_m) of all four DNA hairpins complexed or not complexed with Zn^{2+}/Mg^{2+} was determined using UV absorption spectroscopy at 260 nm. Four hundred microliters of a 2.5 μM solution of the annealed hairpins in M-DNA buffer in the presence or absence of 0.5 mM Zn^{2+} (or Mg^{2+}) were analyzed using a Beckman Coulter DU-800 UV–Vis spectrophotometer in the temperature region 20–85°C. Temperature was increased at a rate of 0.5°C/min. Melting temperatures were determined from the first derivative of the hyperchromicity profiles except for the 3′-FdU and 5′-FdU samples in the presence of Zn^{2+} for which an inflection point was not observed, consistent with strand slippage during melting, and the T_m calculated from the percent increase in hyperchromicity (Supplementary Figure S4).

Cytotoxicity of FdU hairpins and Zn^{2+} complexes

The cytotoxicity of the FdU hairpins and Zn^{2+} complexes was determined using a modified clonogenic assay with an MTT read-out. PC3 prostate cancer cells were seeded in 24-well plates at a cell density of 250 cells/well with 500 μl complete media (Roswell Park Memorial Institute (RPMI) + 10% fetal bovine serum (FBS) + 1% Penicillin & Streptomycin). After 24 h, media was removed and cells were washed twice with 500 μl phosphate-buffered saline (PBS) followed by addition of 500 μl serum-free RPMI. The 3′-FdU–Zn^{2+} complex was formed by incubating 100 μM 3′-FdU hairpin with 5 mM Zn^{2+} in M-DNA buffer at room temperature for 1 h. Lipofectamine 2000 (Invitrogen) was diluted in 100 μl Opti-MEM media (pH = 8.0) to 7.5 ng/μl and incubated at room temperature for 5 min. The 3′-FdU–Zn^{2+} complex was then combined with diluted lipofectamine and incubated at room temperature for 20 min followed by the addition to each well. After 12 h, media was replaced with fresh complete media and incubated at 37°C for a total of 14 days with media changes every 2 days. Cell viability was then assessed using an MTS assay. All experiments were done in triplicate. Each set of data (net absorbance) were then expressed as a percentage, considering the no treatment (i.e., lipofectamine only) group as 100%.

Computational modeling

The initial models for the Zn^{2+} complexes were derived from coordinates for two consecutive dT–dA base pairs extracted from the NMR solution structure (pdb 1JVE) (13). Conversion to FdU was performed by deleting the thymidine methyl group and replacement with fluorine. Initially, eight complexes were geometry optimized in the absence of Zn^{2+} and water molecules: (i) fully protonated: both thymidine (or FdU) base nitrogens protonated; (ii) hemi-deprotonated: one protonated thymidine (or FdU) base nitrogen and one unprotonated thymidine (or FdU) base nitrogen; (iii) fully deprotonated: two unprotonated thymidine (or FdU) base nitrogens. There are two non-identical hemi-deprotonated complexes: (i) 5′-dT-(or 5′-FdU-) deprotonated or (ii) 3′-dT-(or 3′-FdU-) deprotonated). Geometry optimizations were performed with the addition of Zn^{2+} and water molecules to each complex. For all calculations, the NMR structure

was used as the starting configuration and two Mg^{2+} counterions were added in the vicinity of the backbone phosphorus. Zn^{2+} was added (except in the control computation) between the fluorine atoms of the two FdU. Additional calculations confirmed the structures obtained were independent of initial Zn^{2+} placement. All modifications were performed using Molden. All structures were geometry optimized with Gaussian 03 using PM3 in Cartesian coordinates. Post-optimization, single-point calculations were performed with a minimal basis set (STO-3g*) to obtain energies and for a Natural Bond Orbital analysis (14) from which the Wieburg bond orders were extracted. Stabilization energies were calculated by subtracting the energy of dA–dT (or FdU) in the appropriate protonation state (doubly, singly or unprotonated) and the energy of Zn^{2+} with four water molecules from the energy of the full complex.

RESULTS

Formation and stability of DNA–Zn^{2+} complexes

The propensity of Zn^{2+} or Mg^{2+} to increase the thermal stability of four DNA hairpin sequences was evaluated by UV hyperchromicity measurements while the propensity of these metal ions to form specific complexes with these DNA hairpin sequences was evaluated using an EtBr exclusion assay. The results of the thermal stability studies are summarized in Table 1 and representative thermal melting graphs are displayed in supplementary data (Supplementary Figure S4). The control (no-FdU) sequence consisting only of native nucleotides (Figure 2) had a melting temperature of 54.3°C in the absence of divalent metal ions. The native sequence was markedly stabilized by Mg^{2+} ($T_m \geq 62.2$°C); however, Zn^{2+} addition resulted in non-equilibrium melting conditions for the native sequence with an unexpectedly low apparent T_m (37.6°C). Mg^{2+} increased the thermal stability of all sequences except Alt–FdU. The extent of stabilization for 3′-FdU or 5′-FdU by Mg^{2+} was, however, not as great as for the native sequence (Table 1). In contrast to the apparent destabilizing effects of Zn^{2+} on the native sequence, Zn^{2+} markedly stabilized both hairpin sequences that contained consecutive FdU nucleotides (3′-FdU and 5′-FdU) (Figure 2). The stabilization of the 3′-FdU and 5′-FdU sequences by Zn^{2+} was slightly greater than the extent of stabilization of the native sequence by Mg^{2+}. Interestingly, a melting temperature for the Alt–FdU sequence could not be obtained in the presence of Zn^{2+} as addition of Zn^{2+}-induced precipitation of the Alt–FdU sample during the thermal melting experiments, likely as a consequence of interstrand complex formation as reported in previous FRET studies (9). Zn^{2+} also qualitatively altered the shape for the thermal melting curves for all four samples, and for 5′-FdU and 3′-FdU the T_m was estimated from the percent change in hyperchromicity rather than from the first derivative of the melting profile (Supplementary Figure S4). The thermal melting results are consistent with selective stabilization of DNA sequences containing consecutive FdU nucleotides by Zn^{2+}.

Table 1. Melting temperatures for DNA hairpins as a function of metal ion

	Zn^{2+}	Mg^{2+}	No metal
3′FdU	66.1	47.4	44.5
5′FdU	60.5	45.0	39.5
Alt FdU	–	44.8	46.4
Control	37.6[a]	62.2	54.3

[a]Value reported is an apparent T_m as addition of $Zn2^+$ resulted in non-equilibrium conditions.

The formation of specific complexes for the four DNA hairpin sequences with Zn^{2+} and with Mg^{2+} was evaluated by measuring the quenching of EtBr fluorescence. The results are summarized in Figure 3. Addition of Mg^{2+} resulted in a slight, concentration-dependent decrease in EtBr fluorescence for all DNA hairpins except Alt–FdU (~85% of control). In contrast, the effects of Zn^{2+} were highly sequence dependent. The effects of Zn^{2+} on the control sequence were similar to the effects of Mg^{2+} with a moderate concentration-dependent decrease in EtBr fluorescence. The effect of Zn^{2+} on the 'Alt–FdU' sequence was also moderate. In contrast, Zn^{2+} had a dramatic effect on EtBr fluorescence for the 3′-FdU and 5′-FdU sequences. Addition of 1 mM Zn^{2+} resulted in attenuation of EtBr fluorescence to <25% of control for these two sequences (Figure 3). The results are consistent with Zn^{2+} forming specific complexes with DNA sequences containing consecutive FdU nucleotides. Similar complexes do not form with Mg^{2+} or with sequences containing non-consecutive FdU nucleotides.

CD of DNA–Zn^{2+} complexes

CD was used to evaluate alterations to DNA structure caused by Mg^{2+} or Zn^{2+} binding. All four DNA hairpins displayed CD spectral features characteristic of B-form DNA (Figure 4). The addition of Zn^{2+}, but not Mg^{2+}, resulted in a concentration-dependent blue-shift of ~20 nm for the maximal positive ellipticity near 280 nm selectively for the DNA sequences containing consecutive FdU nucleotides. The CD spectra for the control sequence consisting of only native nucleotides displayed no significant variability upon addition of either Mg^{2+} or Zn^{2+} (Figure 4). The maximal ellipticity at 280 nm depends on base pairing, base stacking and base tilting, and shifts in this maximum for the FdU-containing sequences are consistent with alterations in local base pair geometry upon Zn^{2+} complex formation.

Molecular modeling Zn^{2+}–DNA complexes

The preferred geometry for Zn^{2+} binding DNA sequences containing consecutive FdU nucleotides was calculated using Gaussian 03. Specifically, the coordinates for two consecutive dT–dA base pairs were extracted from the NMR solution structure for a DNA hairpin similar to those used for the present studies (pdb 1JVE) (13). Thymidine methyl groups were replaced with fluorine. The geometry and charge distribution for the 2 bp duplex was optimized under three conditions: (i) 'high pH state' in which both FdU were ionized (−1 net charge on each nucleobase); (ii) 'biological pH state' in

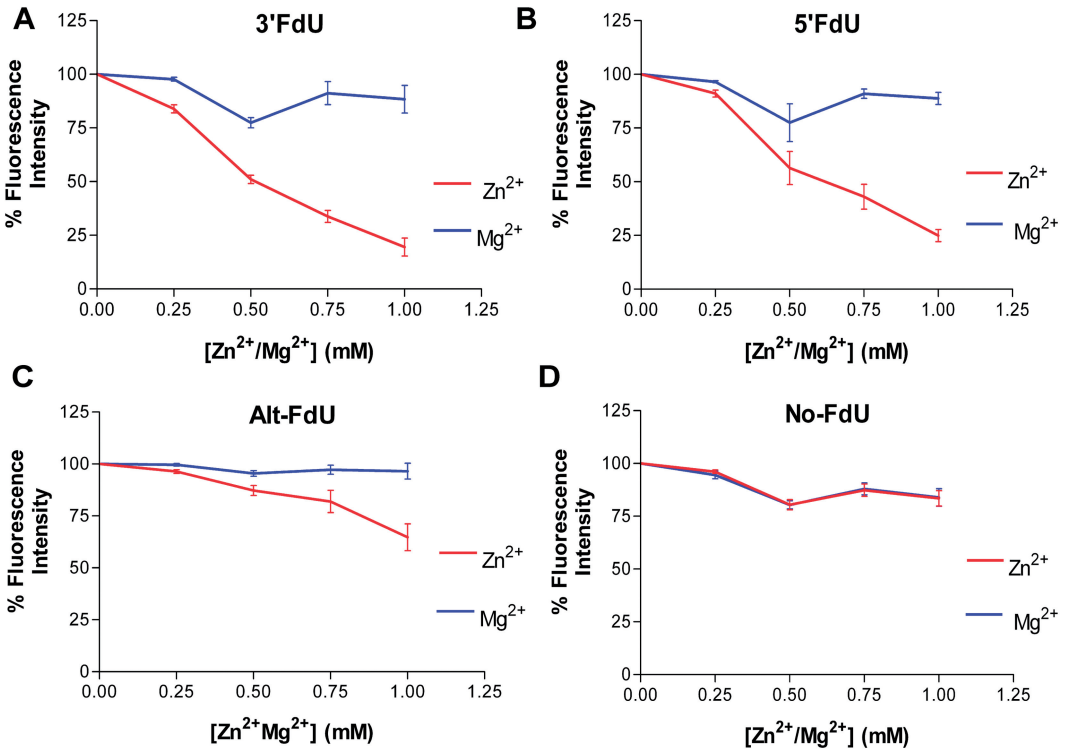

Figure 3. Zn^{2+}, but not Mg^{2+}, inhibits EtBr intercalation into duplex DNA containing consecutive FdU–dA base pairs. EtBr exclusion data are shown for each of the four DNA hairpins in the presence of the indicated concentrations of Zn^{2+} (red) or Mg^{2+} (blue). (**A**) 3′FdU hairpin; (**B**) 5′ FdU hairpin; (**C**) Alt-FdU hairpin; (**D**) No-FdU sequence.

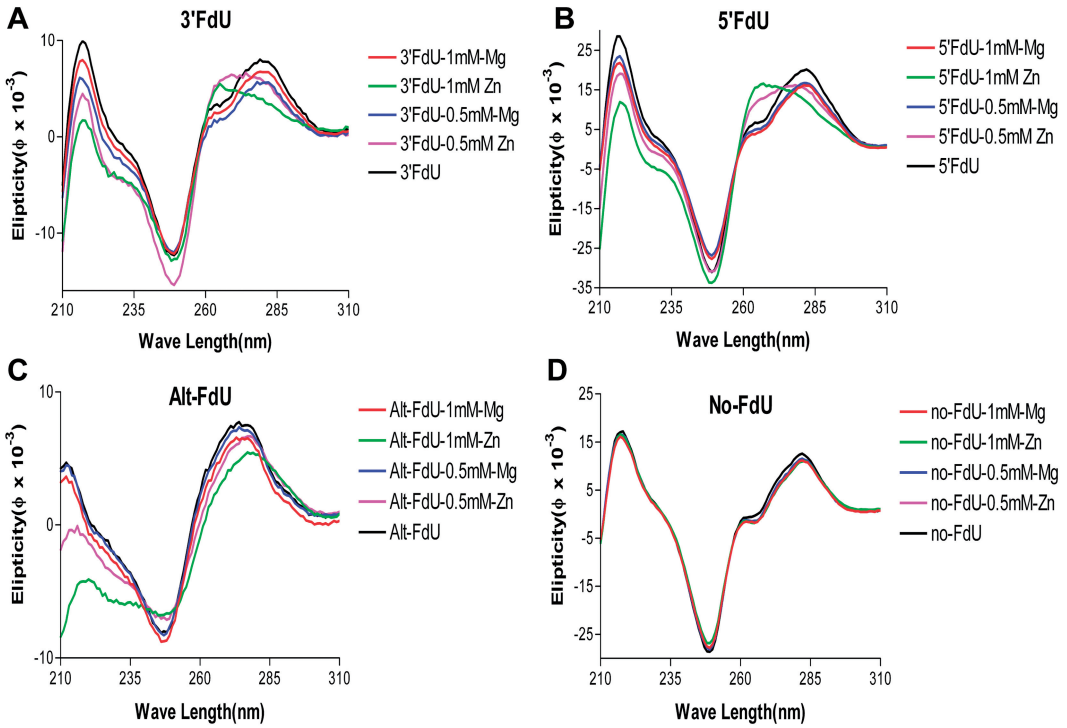

Figure 4. CD spectra demonstrate Zn^{2+} selectively induces a hypsochromic shift upon addition to DNA hairpins containing consecutive FdU–dA base pairs. Spectra for each hairpin were acquired in the presence and absence of Zn^{2+} and Mg^{2+} at the indicated concentrations. The CD spectra indicate that complexation with Zn^{2+} alters the structure of DNA hairpins that contain consecutive FdU–dA base pairs. Computational studies indicate base slide and tilt accompany Zn^{2+} complexation (Figure 1B). (**A**) 3′FdU hairpin; (**B**) 5′ FdU hairpin; (**C**) Alt-FdU hairpin; (**D**) No-FdU sequence.

which one FdU was ionized (pK_A of FdU ~7.6) and (iii) a 'low pH state' in which neither FdU was ionized. Zn^{2+} was added to the system and the overall geometry and charge distribution were optimized for minimal energy as described in the methods. The structure of the dinucleotide step under biological pH conditions (i.e. hemi-deprotonated) with the addition of water molecules to coordinate Zn^{2+} is shown in Figure 1. Surprisingly, Zn^{2+} is located in the major groove with simultaneous interactions with the O4 carbonyl oxygen of the 3′-terminal FdU and F5 of the 5′-terminal FdU, which is deprotonated in the low energy structure. The Zn^{2+}–F distance is 3.2 Å while the Zn^{2+}–O4 distance is 1.9 Å. The Zn^{2+}–O4 interaction has a bond order of 0.277 and thus is a partial covalent bond (Supplementary Table S3). Zn^{2+} significantly stabilized the biological pH structure with stabilization energy of 3.84 kcal/mol. Zn^{2+} coordinates three water molecules with distances of 2.10, 2.12, and 2.14 Å. The overall coordination geometry for Zn^{2+} is distorted trigonal bipyramidal. A similar geometry is observed in the high pH [fully deprotonated state (Supplementary Figure S1)]. In the 'low pH state', Zn^{2+}, unsurprisingly, does not coordinate with FdU stably, but remains coordinated with the three water molecules. The computational model predicts longer than expected hydrogen bonds for the Watson–Crick base pair maintained in the hemi-deprotonated complex (Supplementary Table S1), likely as a result of an absence of base stacking in the dinucleotide step modeled relative to the complete hairpin for which experimental NMR data indicate maintenance of normal Watson–Crick base pairing.

NMR spectroscopy

The effects of Zn^{2+} complex formation on the structure of the 3′-FdU sequence were analyzed using NMR spectroscopy. ^1H NMR spectra were obtained in 90% H_2O solution. Imino ^1H signals were readily apparent for the 3′-FdU hairpin in the presence of Zn^{2+}, Mg^{2+} and no divalent metal at both pH 7 (Supplementary Figure S5) and pH 8 (Figure 5). Interestingly, although the pK_A for monomeric FdU is ~7.6, there was little change in relative intensity for the FdU imino ^1H between pH 7 and pH 8 either in the no metal sample or in the sample that contained Mg^{2+}. Integration of the FdU imino region was performed relative to a region of carbon bound ^1H (5.8–8.5 ppm) that was indistinguishable in all samples and arbitrarily set to 100. The well-resolved G-imino at 12.5 ppm varied from 0.81 to 1.60 in all samples relative to this standard while integral values ranged from 5.7 to 6.0 for the 10 FdU imino ^1H in this region. End-fraying causes the almost complete loss of the terminal FdU imino ^1H and chemical exchange with water is likely responsible, in part, for the integral values being significantly less than the theoretical value of nine. Thus, for the no metal and Mg^{2+} samples, the FdU imino are mostly protonated and do not titrate significantly between pH 7 and 8.

In contrast to the no metal and Mg^{2+} samples, the integral values for the FdU imino ^1H region for the Zn^{2+} complex display a marked pH dependence. The integral value of 5.87 at pH 7 for the Zn^{2+} sample is similar to that

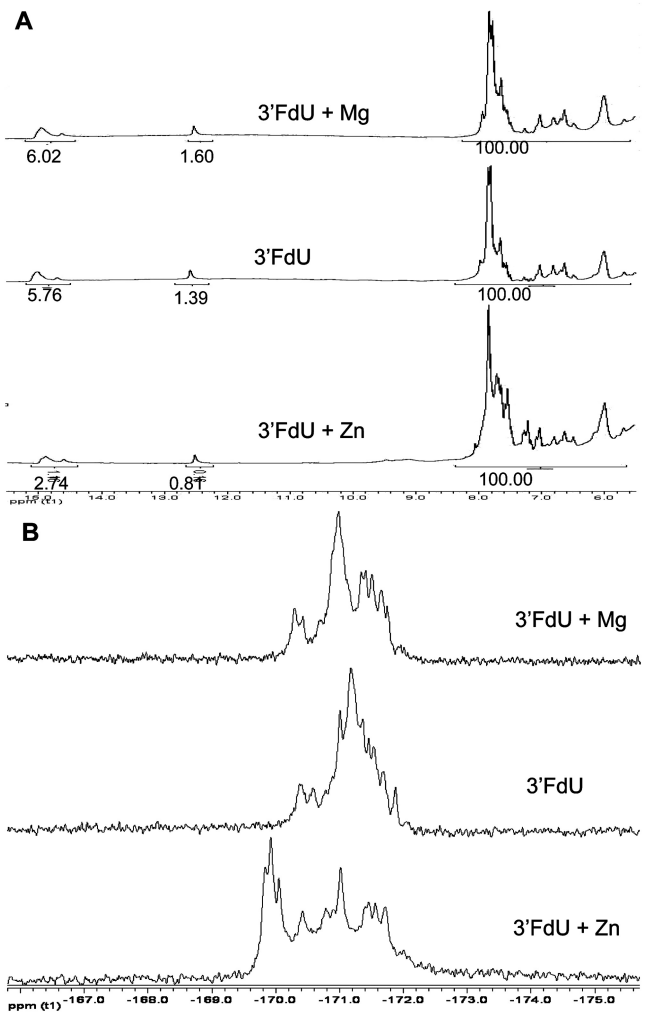

Figure 5. (**A**) ^1H NMR spectra showing no significant intensity change for the imino region for the 3′-FdU hairpin in the presence of Zn^{2+} or Mg^{2+}; (**B**) ^{19}F NMR spectra showing that Zn^{2+}, but not Mg^{2+}, results in significant downfield shifts.

observed for the no metal and Mg^{2+} samples and likely indicates a mostly protonated state for the FdU imino ^1H. EtBr is not excluded from the 3′-FdU in the presence of Zn^{2+} at pH 7. At pH 8, the integral value for the FdU imino ^1H region decreases to 2.74, about one-half of the value observed at pH 7. Under these conditions, the 3′-FdU forms a specific complex with Zn^{2+} that excludes EtBr. Thus, Zn^{2+} perturbs the equilibrium to favor a partly deprotonated state (e.g. hemi-deprotonated) and forms a specific complex with the 3′-FdU hairpin. This complex formation occurs with no discernible changes in chemical shift, only in intensity, for the FdU imino ^1H, indicating the overall structure of the DNA does not undergo major conformational change consistent with the CD data.

In contrast to the relatively minor changes in chemical shift observed for imino ^1H resonances in the presence of Zn^{2+}, ^{19}F NMR spectra displayed significant downfield shifts in the presence of Zn^{2+} at pH 8 (Supplementary Figure 5B) but not pH 7 (Supplementary Figure S5).

The entire ^{19}F region was downfield shifted by 0.2–0.5 ppm and increased spectral dispersion was also evident in the presence of Zn^{2+}. These results are consistent with the computationally derived structure in which one fluorine is an axial ligand for Zn^{2+}. The ^{19}F resonances were not shifted by Mg^{2+} (Supplementary Figure 5B). Since the calculations also indicated Zn^{2+} interacted with an O4 carbonyl oxygen, the one dimensional ^{13}C spectrum was also acquired. Detectable downfield chemical shift changes were observed for resonances having chemical shifts consistent with the C4 carbonyl position (~160 ppm) (Supplementary Figure S6). No other significant changes were evident in the 1D ^{13}C NMR spectrum. The ^{19}F and ^{13}C NMR results are consistent with the structural calculations indicating Zn^{2+} interacts with O4 and F5 of consecutive FdU nucleotides. In contrast to the ^{19}F and ^{13}C spectra in which Mg^{2+} had no significant effect, Mg^{2+}, but not Zn^{2+}, resulted in marked sharpening of the ^{31}P resonances and some increase in spectral dispersion (Supplementary Figure S7).

Cytotoxicity of DNA–Zn^{2+} to PCa cells

Although normal prostate tissue has the highest Zn^{2+} concentration in the human body, prostate cancer (PCa) cells have extremely low intracellular Zn^{2+} and Zn^{2+} is highly cytotoxic to PCa cells (15). Thus, Zn^{2+} complexes of FdU-containing DNA sequences may be cytotoxic to PCa cells both from the intracellular release of Zn^{2+} and from the release of the cytotoxic nucleotide analog FdUMP (6,7). The 3′-FdU DNA hairpin was prepared with and without Zn^{2+} using lipofectamine to promote cellular internalization. Cytotoxicity was evaluated using a modified clonogenic assay with an MTS readout. The results are shown in Figure 6. As is evident from the data, the 3′-FdU hairpin sequence is cytotoxic toward PCa cells. The lipofectamine complex containing Zn^{2+}, but did not include the FdU-substituted DNA, was also cytotoxic toward PCa cells. The cytotoxicity of the Zn^{2+}–DNA complex prepared with lipofectamine displayed the greatest cytotoxicity toward PC3 cells (Figure 6). All samples were prepared under identical conditions. We conclude that inclusion of Zn^{2+} in lipofectamine complexes of FdU-containing DNA sequences enhances the cytotoxicity of FdU-substituted DNA toward prostate cancer cells.

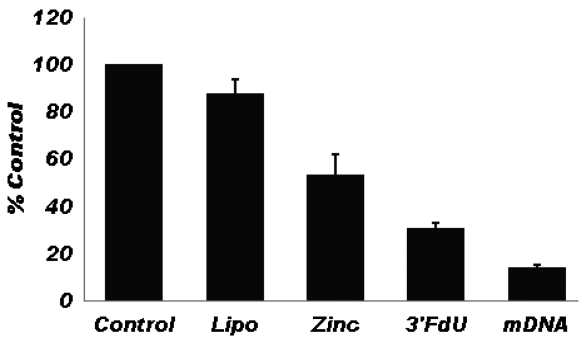

Figure 6. MTS assay results demonstrating the cytotoxicity of Zn^{2+}, the 3′-FdU DNA hairpin and the Zn^{2+} complex of the 3′-FdU hairpin, towards PC3 prostate cancer cells. The Zn^{2+}–DNA complex (mDNA) displays the greatest cytotoxicity.

DISCUSSION

The present work demonstrates that Zn^{2+} forms specific complexes with duplex DNA sequences containing consecutive FdU nucleotides. The evidence for complex formation includes significant increase in thermal stability and exclusion of EtBr intercalation. The effects of Zn^{2+} are highly specific for DNA duplexes containing consecutive FdU nucleotides and do not occur for analogous sequences that contain similar numbers of FdU in non-sequential positions nor occur for sequences consisting of native nucleotides. While Mg^{2+} was found to stabilize all of the DNA hairpins included in the present study except Alt-FdU, stabilization by Mg^{2+} was greatest for the sequence consisting of only native nucleotides. Further, Mg^{2+} was not as efficient as Zn^{2+} at stabilizing DNA sequences that included consecutive FdU nucleotides. Mg^{2+} was also not as effective as Zn^{2+} at excluding EtBr binding to DNA sequences containing consecutive FdU nucleotides. Thus, Zn^{2+} interacts with DNA sequences containing consecutive FdU nucleotides in a manner that is distinct from Mg^{2+}.

Although previous reports have indicated that Zn^{2+} causes intermolecular aggregates from DNA containing alternating FdU–dA at basic pH, the present work is the first to demonstrate that intramolecular complex formation with Zn^{2+} occurs for DNA hairpins containing consecutive FdU nucleotides. As complex formation was not observed with the corresponding dT hairpin DNA sequences and is pH dependent, it is likely that Zn^{2+} preferentially interacts, in part, with ionized FdU nucleotides. Specific interaction of Zn^{2+} with the O2 carbonyl would place Zn^{2+} in the minor groove, a location that has been demonstrated to bind Na^{+} ions in other A–T rich DNA sequence (10). The basis for the requirement of Zn^{2+} binding to DNA sequences that include consecutive FdU nucleotides was elucidated from *ab initio* and semi-empiricial Gaussian calculations that demonstrated, for the first time, that Zn^{2+} coordinates with F5 of the 5′-FdU nucleotide and the O4 carbonyl oxygen of the 3′-neighboring FdU. Activation of F5 for Zn^{2+} complexation requires FdU deprotonation, while the O4–Zn^{2+} interaction occurs with minimal disruption to Watson–Crick geometry. The overall geometry of Zn^{2+} in complex with consecutive FdU nucleotides is trigonal bipyramidal and the ligands not donated by FdU (e.g. F5 and O4) are occupied by water molecules. This mode of Zn^{2+} binding with nucleic acids has not been described previously and is distinct from the binding mode postulated previously in which Zn^{2+} replaced hydrogen in A–FdU base pairs (4,5).

The unique binding mode of Zn^{2+} identified in the present studies is supported by all of the spectral data.

First, the binding motif is consistent with the EtBr exclusion data as interactions of positively charged Zn^{2+} with consecutive nucleotides would be expected to exclude positively charged EtBr from intercalating into the duplex. The computationally preferred Zn^{2+} binding motif is also consistent with all of the ^{1}H, ^{19}F, ^{31}P and ^{13}C NMR data as well as the CD data. In contrast to previous studies that indicated imino ^{1}H were not evident in Zn^{2+} complexes of FdU-containing DNA sequences (4,5), the present study demonstrated Zn^{2+} complex formation occurred under conditions when about one-half the FdU imino ^{1}H were present (e.g., hemi-deprotonated). Thus, under the solution conditions employed in these studies, the FdU nucleotides are not uniformly ionized, Zn^{2+} does not mediate base pair formation and A-FdU base pairing is present although reduced in intensity. The ^{19}F spectra, however, show a downfield shift upon Zn^{2+} complex formation. No changes in the ^{19}F spectra occurred upon addition of Mg^{2+}. The observed downfield shift is consistent with reduced electron density about ^{19}F in the Zn^{2+} complex. ^{19}F resonances are very sensitive to electronic perturbations and while the observed downfield shift for these resonances does not prove a direct interaction between Zn^{2+} and F5 as predicted by the calculations, the observed chemical shifts are consistent with such an interaction. Downfield shifts in the ^{13}C resonances for the C4 carbonyl region of FdU nucleotides were also observed following Zn^{2+} complex formation consistent with the computationally-derived low energy structure. In contrast, Mg^{2+} induced significant chemical shift perturbations to the ^{31}P NMR spectra while Zn^{2+} did not. Thus, all of the NMR spectral data are consistent with the computationally derived binding mode for Zn^{2+} with DNA sequences including consecutive FdU nucleotides.

The present study has demonstrated a previously uncharacterized binding mode for Zn^{2+} with DNA sequences that include consecutive FdU nucleotides. Zn^{2+} binding is energetically favored under conditions where half of the FdU are deprotonated, or slightly above physiological pH (the pK_A of FdU is $\sim$7.6). As both Zn^{2+} and FdU-containing DNA are cytotoxic toward prostate cancer cells, it is of interest whether Zn^{2+} might be complexed with FdU-containing DNA for therapeutic purposes (16). In the present study, we have demonstrated that lipofectamine enhances the cytotoxicity of Zn^{2+}–DNA complexes towards PCa cells. The lipofectamine-stabilized Zn^{2+}–DNA complexes demonstrate enhanced cytotoxicity relative to the components under standard tissue culture conditions. As both Zn^{2+} and FdU-containing DNA are well-tolerated *in vivo*, the complexes are likely to be well-tolerated *in vivo* as well, and may provide a new and more efficacious approach to prostate cancer treatment.

SUPPLEMENTARY DATA

Supplementary Data are available at NAR Online.

ACKNOWLEDGEMENTS

The authors acknowledge Dr Marcus Wright for help with acquisition of ^{31}P and ^{19}F NMR data and Bree Berry and Dr Evan Gomes for technical assistance. All calculations were performed on the DEAC cluster which is supported by WFU Information systems and the WFU Provost's office.

FUNDING

Department of Defense Prostate Cancer Research Program (093606 to W.H.G.); National Institutes of Health (CA102532 to W.H.G.); The North Carolina Biotechnology Center (2P30 CA12197-32); National Institutes of Health (CA12937 and P30 CA12197-32 to F.R.S.). Funding for open access charge: National Institutes of Health (NCI CA102532 DOD CDMRP 093606).

Conflict of interest statement. There is a potential conflict of interest in that Dr Gmeiner is the primary owner of Salzburg Therapeutics which holds the licenses to FdUMP [N] technology.

REFERENCES

1. Liang,J.Y., Liu,Y.Y., Zou,J., Franklin,R.B., Costello,L.C. and Feng,P. (1999) Inhibitory effect of zinc on human prostatic carcinoma cell growth. *Prostate*, **40**, 200–207.
2. Uzzo,R.G., Leavis,P., Hatch,W., Gabai,V.L., Dulin,N., Zvartau,N. and Kolenko,V.M. (2002) Zinc inhibits nuclear factor-kappa B activation and sensitizes prostate cancer cells to cytotoxic agents. *Clin. Cancer Res.*, **8**, 3579–3583.
3. Shi,Y., Beger,R.D. and Berg,J.M. (1993) Metal binding properties of single amino acid deletion mutants of zinc finger peptides: studies using cobalt(II) as a spectroscopic probe. *Biophys. J.*, **64**, 749–753.
4. Lee,J.S., Latimer,L.J. and Reid,R.S. (1993) A cooperative conformational change in duplex DNA induced by Zn2+ and other divalent metal ions. *Biochem. Cell Biol.*, **71**, 162–168.
5. Wood,D.O., Dinsmore,M.J., Bare,G.A. and Lee,J.S. (2002) M-DNA is stabilised in G*C tracts or by incorporation of 5-fluorouracil. *Nucleic Acids Res.*, **30**, 2244–2250.
6. Liao,Z.Y., Sordet,O., Zhang,H.L., Kohlhagen,G., Antony,S., Gmeiner,W.H. and Pommier,Y. (2005) A novel polypyrimidine antitumor agent FdUMP[10] induces thymineless death with topoisomerase I-DNA complexes. *Cancer Res.*, **65**, 4844–4851.
7. Bijnsdorp,I.V., Comijn,E.M., Padron,J.M., Gmeiner,W.H. and Peters,G.J. (2007) Mechanisms of action of FdUMP[10]: metabolite activation and thymidylate synthase inhibition. *Oncol. Rep.*, **18**, 287–291.
8. Gmeiner,W.H., Reinhold,W.C. and Pommier,Y. (2010) Genome-Wide mRNA and microRNA profiling of the NCI 60 cell-Line screen and comparison of FdUMP[10] with fluorouracil, floxuridine, and topoisomerase1 poisons. *Mol. Cancer Ther.*, **9**, 3105–3114.
9. Spring,B.Q. and Clegg,R.M. (2007) Fluorescence measurements of duplex DNA oligomers under conditions conducive for forming M-DNA (a metal-DNA complex). *J. Phys. Chem. B.*, **111**, 10040–10052.
10. Cesare Marincola,F., Denisov,V.P. and Halle,B. (2004) Competitive Na(+) and Rb(+) binding in the minor groove of DNA. *J. Am. Chem. Soc.*, **126**, 6739–6750.

11. Valentina Tereshko,G.M. and Martin,E. (1999) A "Hydrat-Ion" spine in a B-DNA minor groove. *J. Am. Chem. Soc*., **121**, 3590–3595.
12. Hirao,I., Kawai,G., Yoshizawa,S., Nishimura,Y., Ishido,Y., Watanabe,K. and Miura,K. (1994) Most compact hairpin-turn structure exerted by a short DNA fragment, d(GCGAAGC) in solution: an extraordinarily stable structure resistant to nucleases and heat. *Nucleic Acids Res*., **22**, 576–582.
13. Ulyanov,N.B., Bauer,W.R. and James,T.L. (2002) High-resolution NMR structure of an AT-rich DNA sequence. *J. Biomol. NMR*, **22**, 265–280.
14. Reed,A.E., Weinstock,R.B. and Weinhold,F. (1985) Natural-population analysis. *J. Chem. Phys*., **83**, 735–746.
15. Ghosh,S.K., Kim,P., Zhang,X.A., Yun,S.H., Moore,A., Lippard,S.J. and Medarova,Z. (2010) A novel imaging approach for early detection of prostate cancer based on endogenous zinc sensing. *Cancer Res*., **70**, 6119–6127.
16. Gmeiner,W.H. (2006) Genetic determinants for activated fluoropyrimidine chemotherapy. *Drug Devel. Res*., **66**, 1–11.